# Enhanced solar photocatalysis of $TiO_2$ nanoparticles and nanostructured thin films grown on paper

NANO EXPRESS

PAPER

# Enhanced solar photocatalysis of $TiO_2$ nanoparticles and nanostructured thin films grown on paper

T Freire[1,2], A R Fragoso[1], M Matias[1,2], J V Pinto[1], A C Marques[1], A Pimentel[1], P Barquinha[1], R Huertas[3], E Fortunato[1], R Martins[1,*] and D Nunes[1,*]

[1] i3N/CENIMAT, Department of Materials Science, Faculty of Sciences and Technology, Universidade NOVA de Lisboa, Campus de Caparica, 2829-516 Caparica, Portugal
[2] AlmaScience Colab Madan ParqueCaparica 2829-516, Portugal
[3] iBET-Instituto de Biologia Experimental e Tecnologica, Oeiras, Portugal
[*] Authors to whom any correspondence should be addressed.

**E-mail:** rm@uninova.pt **and** daniela.gomes@fct.unl.pt

**Keywords:** $TiO_2$ nanoparticles, nanostructured films, paper substrates, photocatalysis, microwave irradiation

OPEN ACCESS

RECEIVED
26 December 2020

REVISED
3 March 2021

ACCEPTED FOR PUBLICATION
9 March 2021

PUBLISHED
22 October 2021



## Abstract

Titanium dioxide nanoparticles and nanostructured thin films were simultaneously synthesized using a microwave-assisted hydrothermal method. The synthesis formed very fine particles, appearing as nanospheres in the 11 nm size range. As for the nanostructured films, they have displayed similar structural characteristics to the nanoparticles, with thickness of 130 nm. These films covered uniformly and homogenously the Whatman paper, while maintaining its flexibility. The materials processed had their photocatalytic activity assessed from rhodamine B degradation under solar radiation (91% degradation after 40 min for the powder material and 68% after 6 h for the nanostructured thin films). Reusability experiments were also carried out, revealing superior performance concerning the Degussa P25, the most common photocatalyst used. The results of the present work can be thought as an option for the existing photocatalysts activated under solar light, namely for water purification, as it simultaneously produces enhanced photocatalytic powders and photocatalytic papers fully disposable and that can be easily recycled.

## 1. Introduction

Water is an essential resource for all known forms of life, and it is used in every industrial sector. Despite covering 70% of the Earth's surface, just 2.5% of this water is fresh for consumption and even this small percentage is not accessible for every human in the planet Earth. This scarcity and misuse led to the necessity to develop techniques and products that facilitated the treatment of wastewater and helped decreasing the amount of people without access to it.

Since the beginning of the millennium, companies and governments [1–4] have been addressing sustainability issues, approaches to decrease the problems caused by human activities and industrial sectors and ways to make responsible choices regarding natural resources' exploitation, which culminated in the Sustainable Development Goals by the UN, such as the Goal 6: Clean Water and Sanitation. To make this possible some metal oxides, like Titanium Dioxide ($TiO_2$), are being used as photocatalytic agents to breakdown different water pollutants.

$TiO_2$ is an environmentally friendly, earth abundant [5], versatile n-type semiconductor used for several applications, like photocatalysis [6–9], dye-sensitized solar cells [10–13], electrochromic devices [13–16], and is even used as an antibacterial agent [17–19]. This material can exhibit different structural phases, being the most common the rutile, anatase and brookite [13, 16, 20], typically $TiO_2$ displaying an optical bandgap of 3.0 and 3.2 eV for rutile and anatase, respectively, and a bandgap for brookite ranging from 3.1 and 3.4 eV [16, 20, 21]. $TiO_2$ is extensively used as a photocatalyst in the forms of anatase, rutile, brookite or as mixed phases [22–25].

Photocatalysis is described as the process of altering reactions' rate upon exposure to a light source. In this process, the material absorbs photons that will give sufficient energy to an electron ($e^-$) in the valence band to get excited and jump to the conduction band, leaving behind a positive charge particle ($h^+$) and generating an electron-hole pair, which will be responsible for reducing and oxidizing the compounds on the photocatalyst surface [26–28]. The water splitting induced by the $TiO_2$ photocatalytic properties is a widely studied phenomenon, in which this material, through the reduction and oxidation of the solution, originates $O_2^{\bullet}$ and $OH^{\bullet}$ radicals that are effective in the decomposition of organic substances, pollutants and microorganisms. In the field of photocatalysis, $TiO_2$ appears as a common solution for several applications related with water treatment since this material displays strong oxidizing abilities for the organic pollutants' decomposition, its hydrophilicity, chemical stability and low cost [29–32].

$TiO_2$ films can be integrated in flexible and rigid substrates and used as water filters. Despite being an efficient process, $TiO_2$ photocatalysis is most likely to be activated by UV irradiation, which only comprises a reduced portion of the solar spectrum. Taking advantage of the rest of the solar spectrum is the future of photocatalysis [8, 27, 33, 34]. Thus, approaches for making $TiO_2$ photoactive under solar radiation are highly sought.

The synthesis method for the $TiO_2$ as a photocatalyst material is a key factor in its final cost and performance and should also take in account the type of substrate used for deposition. Several methods have been reported in the literature for the production of $TiO_2$ films for photocatalytic applications, including CVD [35, 36], spray pyrolysis [35, 37], sol-gel [35, 38], hydrothermal synthesis [35, 39], and microwave-assisted synthesis [7, 35, 40]. The latter synthesis route enables the use of flexible substrates, like paper [6, 14], and allows reproducibility while being an inexpensive, fast and simple method.

The following study will describe the synthesis and further characterization of $TiO_2$ nanoparticles and nanostructured thin films grown on paper and produced simultaneously by microwave-assisted hydrothermal technique. The main goal was the production of stable, environmentally friendly, and cost-effective $TiO_2$ materials with improved photocatalytic behaviour under solar radiation, and also achieving an enhanced disposable photocatalytic paper.

## 2. Experimental procedure

### 2.1. Materials

Both $TiO_2$ nanoparticles and nanostructured thin films were synthesized simultaneously using a microwave-assisted hydrothermal method. The materials were produced at least 3 times to demonstrate the technique reproducibility. The $TiO_2$ synthesis used deionized water, titanium (IV) isopropoxide ($Ti[OCH(CH_3)_2]_4$, TTIP, 97% from Sigma Aldrich), and hydrochloric acid (HCl, 37% from Merck). For the microwave synthesis, it has been mixed 57.5 ml of water on 2.5 ml of HCl under stirring during 5 min 2 ml of TTIP was then added to the solution and stirred for 10 min prior to synthesis. A CEM Focused Microwave Synthesis System (CEM Discover SP) was used in this work. The microwave parameters were set at 75 min, 100 W, 110 °C and 200 Psi, for synthesis time, power, temperature, and pressure, respectively. Quartz vessels of 35 ml were used, and a piece of the Whatman substrate was added for the $TiO_2$ film to grow. Afterwards, 20 ml of the mixed solutions were transferred into it. The microwave parameters selected have been previously employed in [6, 14, 41]. when using paper as substrate.

The substrate used was the Whatman chromatography paper grade 2 with sizes of $2 \times 2.5\ cm^2$. The selection of this paper was due to the absence of impurities or additives associated to its uniform hydrophilic properties [6, 42]. There was no need of a seed layer to assist $TiO_2$ growth [6].

### 2.2. Characterization techniques

The x-ray diffraction (XRD) measurements were achieved using a diffractometer PANalytical's X'Pert PRO MPD equipped with a X'Celerator 1D detector and using CuK$\alpha$ radiation. XRD diffractograms were recorded in the 20–75° $2\theta$ range with a step size of 0.033°. The rutile, anatase, brookite simulated powder diffractograms were obtained using PowderCell [43] and crystallographic data from [44].

Raman spectroscopy measurements were carried out using an inVia Qontor confocal Raman microscope from Renishaw. It has been used a 17 mW He–Ne laser operating at 532 nm, with a 10 s exposure time and settings of 3 accumulations. The Raman spectra were recorded in the range of 100–700 $cm^{-1}$.

Surface scanning electron microscopy (SEM) images were obtained with a Carl Zeiss AURIGA CrossBeam SEM-FIB microscope equipped for energy dispersive x-ray spectroscopy (EDS) analyses. The nanoparticles and films' dimensions have been estimated using SEM images and ImageJ software [45].

The optical bandgap was estimated through diffuse reflectance measurements carried out at room temperature using a Perkin Elmer lambda 950 UV/VIS/NIR spectrophotometer equipped with a diffuse

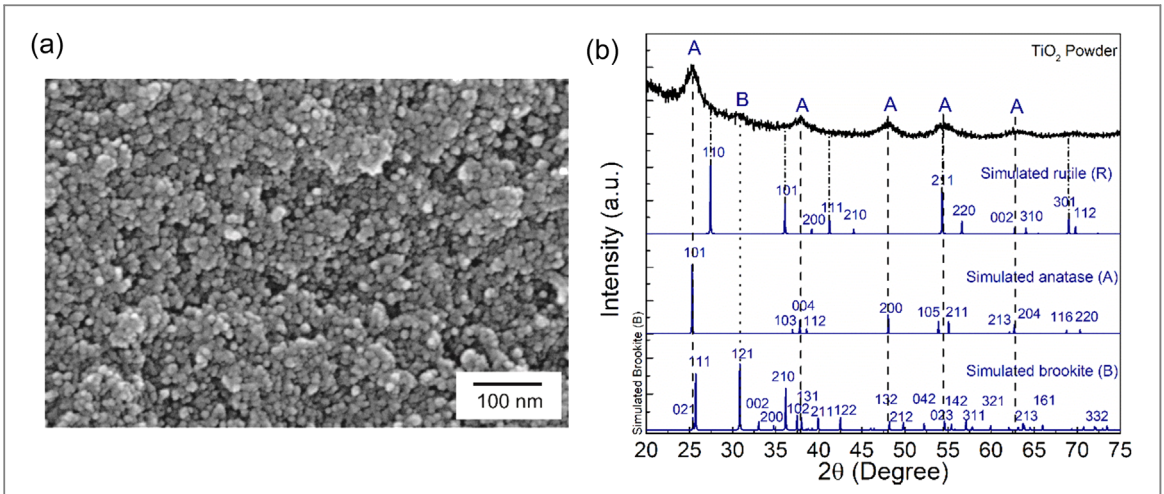


**Figure 1.** SEM image of the $TiO_2$ nanoparticles (a) together with its XRD diffractogram (b), where the simulated rutile, brookite and anatase diffractograms are presented for comparison.

reflectance module (integrating sphere with 150 mm diameter and internally coated with Spectralon). A standard reflector sample was used calibration (reflectance, R = 1.00 from Spectralon disk). The reflectance (R) measurements were carried out from 250 to 800 nm.

### 2.3. Photocatalysis experiments

The $TiO_2$ nanoparticles and nanostructured thin film had their photocatalytic behaviour assessed by the photodegradation of rhodamine B (RhB) from Sigma-Aldrich at room temperature. The samples were positioned at the bottom of a beaker with 50 ml of the RhB solution (20 mg $l^{-1}$) and left to stir for 30 min in the dark to establish absorption–desorption equilibrium. Absorbance measurements were taken every 10 min up to 70 min in the case of powder materials, and every 2 h up to a total of 6 h in the case of paper-based materials, using Shimadzu UV-3101PC UV–vis-NIR Scanning Spectrophotometer. For powder materials, 4 ml of the rhodamine B solution with the photocatalyst was collected after light exposure and separated by centrifugation for 5 min at 6000 rpm. After absorbance measurements, the 4 ml solution was returned for further measurements. The reusability experiments consisted in recovering the powder and centrifuging it with further discard of the total liquid. The recovered slurry was dried at 50 °C for 3 h. The recovered dried powder was then poured into fresh solution and exposed to solar light for 70 min along several weeks [22]. The commercial Degussa P25 $TiO_2$ was tested in the same proportion as the produced powders (20 mg $l^{-1}$).

The irradiation was achieved by using a LED solar simulator LSH-7320 (AM 1.5 spectrum) with an intensity of 1 Sun, and the photocatalytic experiments considered the International Standard ISO 10678 [46].

## 3. Results and discussion

$TiO_2$ nanoparticles and the nanostructured $TiO_2$ thin film were successfully synthesized under microwave irradiation using a cellulose-based substrate. i.e., Whatman paper. The produced nanostructures and thin film were systematically investigated and correlated to their final photocatalytic behaviour under solar radiation. All samples showed that the process is reproducible and reliable, where deviations observed on the set of the materials' characteristics analysed were below 4% and 10% for the powder and thin films, respectively. The approach presented opens-up to the simultaneous production of photocatalytic powders and disposable photocatalytic paper activated under solar light.

### 3.1. Structural characterization

Figure 1(a) depicts the SEM images of $TiO_2$ nanoparticles. The microwave synthesis resulted in very fine particles, appearing as nanospheres. These nanoparticles appear in an agglomerate, since after drying the powder there is aggregation in larger particles in the micrometer range. The average sphere diameter calculated was 11 ± 0.5 nm. The powder produced was also analysed by x-ray diffraction and the XRD diffractograms are presented in figure 1(b). Most peaks of the experimental diffractogram could be assigned to the anatase phase, nevertheless the presence of brookite could also be observed (as a minor second phase or impurity). It has not been detected peaks coming from impurities such as $Ti(OH)_4$ and the XRD results demonstrate that the materials are well crystallized and highly nanostructured. This mixture of phases was previously reported with

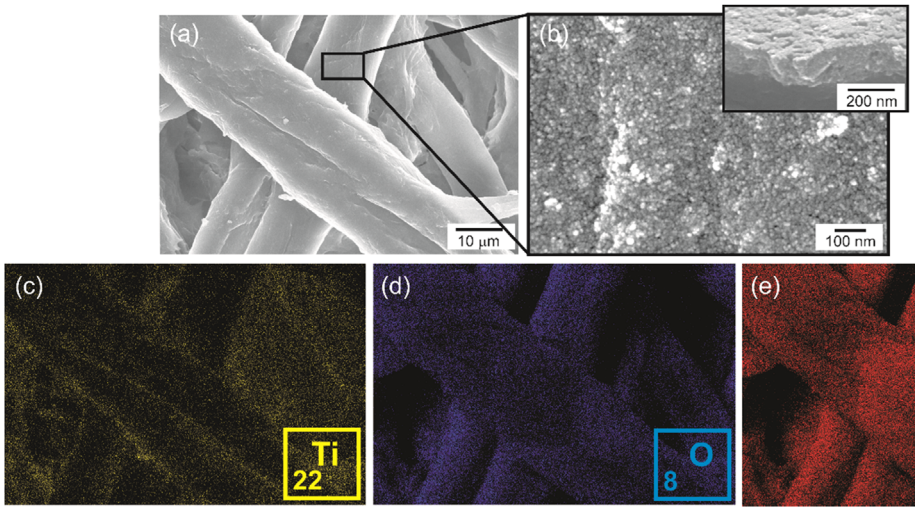


**Figure 2.** SEM and EDS analysis on the $TiO_2$ nanostructured thin film grown on Whatman paper.

small amounts of brookite in $TiO_2$ anatase nanocrystals when synthesized by hydrothermal synthesis [47]. The mean particle size calculated from Scherrer's equation was 5 nm [48]. In analogous studies, HCl played a central role in the determination of the final $TiO_2$ crystalline phase. Both studies reported the presence of a mixture of rutile and brookite when using higher amounts of acid [14, 22]. When comparing with [14], where 5 ml of HCl has been used, it can be concluded that after a certain amount of acid, the formation of anatase phase is preferred. In the present work, 2.5 ml of HCl resulted in mostly anatase with residual presence of brookite.

In figures 2(a) and (b) it is presented the SEM images of the $TiO_2$ nanostructured films grown on the Whatman paper substrate without any seed layer. The paper roughness promoted nucleation and fixation of the $TiO_2$ nanostructures without any additional process [6, 14, 41]. After microwave synthesis, the Whatman paper fibres remain unaltered, and when magnifying the observed area, it is clear the presence of nanostructures forming a continuous film. The nanoparticles resultant from the microwave synthesized powder uniformly covered the paper substrate. The inset shows the cross section of the film, and it could be observed a compact film of agglomerated nanoparticles, with thickness around 130 nm. From EDS analysis, it can be observed the homogenous distribution of Ti within the substrate (figure 2(c)), together with the presence of C and O (figures 2(d) and (e)), where C is related to the use of a paper substrate. No impurities were detected.

From previous studies, it has been concluded that paper hinders the $TiO_2$ signal on XRD measurements [6, 14], and for that reason Raman spectroscopy has been employed. The Raman spectra of the $TiO_2$ nanoparticles and the thin film grown on Whatman paper are presented in figure 3. The Raman spectrum of the pristine Whatman paper is also shown for comparison, and the minor bands marked with the star are associated to the substrate. The Raman spectra attested for the presence of the anatase and brookite phases (more evident in the powder Raman spectrum). The Raman bands associated to anatase were detected with a blue shift and can be assigned to 153 $cm^{-1}$ ($E_g$), 204 $cm^{-1}$ ($E_g$), 405 $cm^{-1}$ ($B_{1g}$), 512 $cm^{-1}$ ($B_{1g} + A_{1g}$), and 640 $cm^{-1}$ ($E_g$) for anatase [47, 49–51]. This Raman band shift can be related to the structural defects present in the $TiO_2$ lattice, oxygen vacancies [47–52] or minor deviations from the $TiO_2$ films' stoichiometry [53]. Some Raman bands associated to brookite have also been observed (246, 322 and 365 $cm^{-1}$ [54, 55]). In fact, the Raman spectra of brookite phase display a characteristic intense band at 153 $cm^{-1}$, which can be similar and coincident with $E_g$ mode of anatase at 144 $cm^{-1}$ [47]. However, being brookite a minor phase or impurity, it can be assumed that the 153 $cm^{-1}$ band comes from anatase phase. XRD measurements on powder confirmed the Raman spectroscopy results (figure 1(b)).

### 3.2. Optical characterization

Both powder and thin film materials had their optical band gap assessed through reflectance data using the Tauc plot [56, 57]. The direct band gap values estimated were 3.07 eV and 3.44 eV for the $TiO_2$ nanoparticles and nanostructured thin film, respectively (figure 4). The estimated band gaps are within the reported values for the different $TiO_2$ phases [21, 58, 59]. Regarding the band gap determination, Reddy *et al* [60] reported both the direct and indirect band gap measurements, being the direct transition more favourable for anatase $TiO_2$ nanoparticles with sizes of 5–10 nm. Moreover, the disparity observed between the powder and the thin film materials is expected since the band gap depends on several factors including defects [61], residual strain [62], degree of compactness and densification [63], among others.

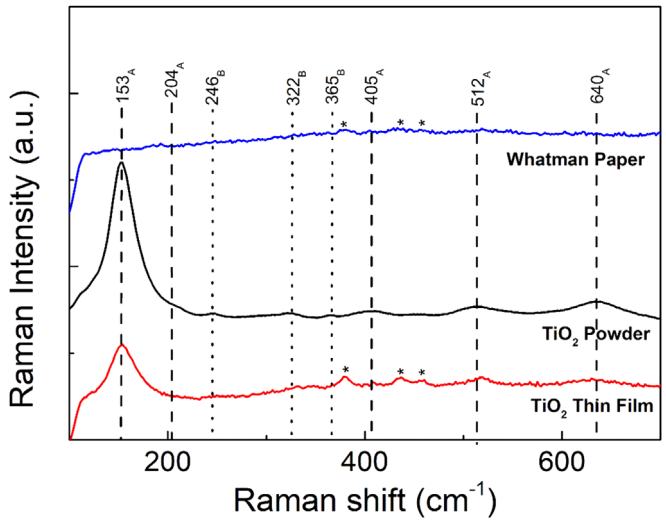


**Figure 3.** Raman spectra of the pristine Whatman paper, $TiO_2$ nanoparticles and nanostructured thin film grown on paper. Dashed lines indicate the anatase bands and the dot ones indicate the brookite bands. The stars represent the contribution from Whatman paper.

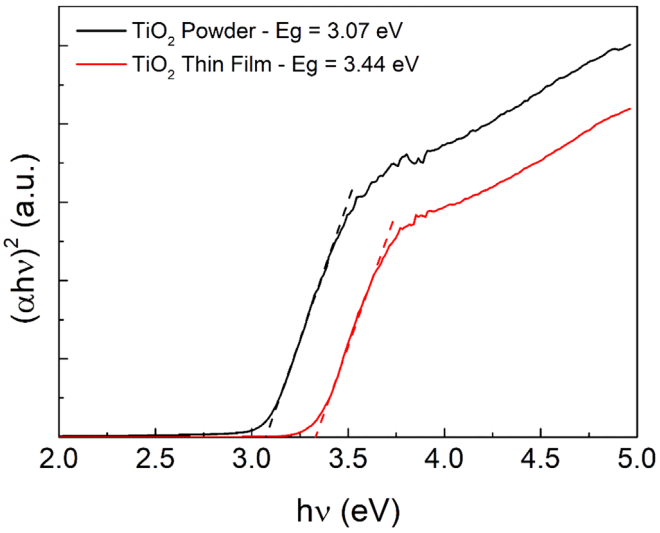


**Figure 4.** Tauc plot ($(\alpha h\nu)^2$ variation versus photon energy $h\nu$) for the $TiO_2$ nanoparticles and nanostructured thin film grown on paper for the evaluation of the materials' optical band gap.

### 3.3. Photocatalytic behaviour

Both $TiO_2$ nanoparticles (powder) and the nanostructured thin film grown on paper had their photocatalytic activity evaluated through the rhodamine B photodegradation under solar radiation. It can be seen the gradual RhB degradation for the powder material (figure 5(a)), reaching degradation values of 91% after 40 min. From 50 min, the reaction has reached a stable degradation pattern, reaching 93% at 70 min (last measurement) for the powder $TiO_2$. The degradation ratio ($C/C_0$) versus exposure time is presented in figure 5(b) for the powder materials, where C is the concentration of the pollutant at each exposure time and $C_0$ is the initial solution concentration. When compared to the $TiO_2$ Degussa P25 catalyst, the synthetized powder revealed an enhanced photocatalytic activity under solar radiation (see figure 5(b)). Pure $TiO_2$ is photo-active under UV radiation, however in the present work, it can be observed an enhanced photocatalytic activity under solar radiation. This behaviour has been reported before and is associated to the presence of nano-sized $TiO_2$ [64]. Other factors also influence the photocatalytic activity and will be discussed in detail.

The photocatalytic activity relies on numerous factors including the band gap, crystallite size, degree of crystallinity, specific surface area, active facets, among others [7, 65, 66]. The band gap estimated for the $TiO_2$ nanoparticles are within what is expected for the different $TiO_2$ phases. Regarding the crystallite size, and as observed in figure 1(a) and calculated by XRD results, the microwave synthesis resulted in very fine particles

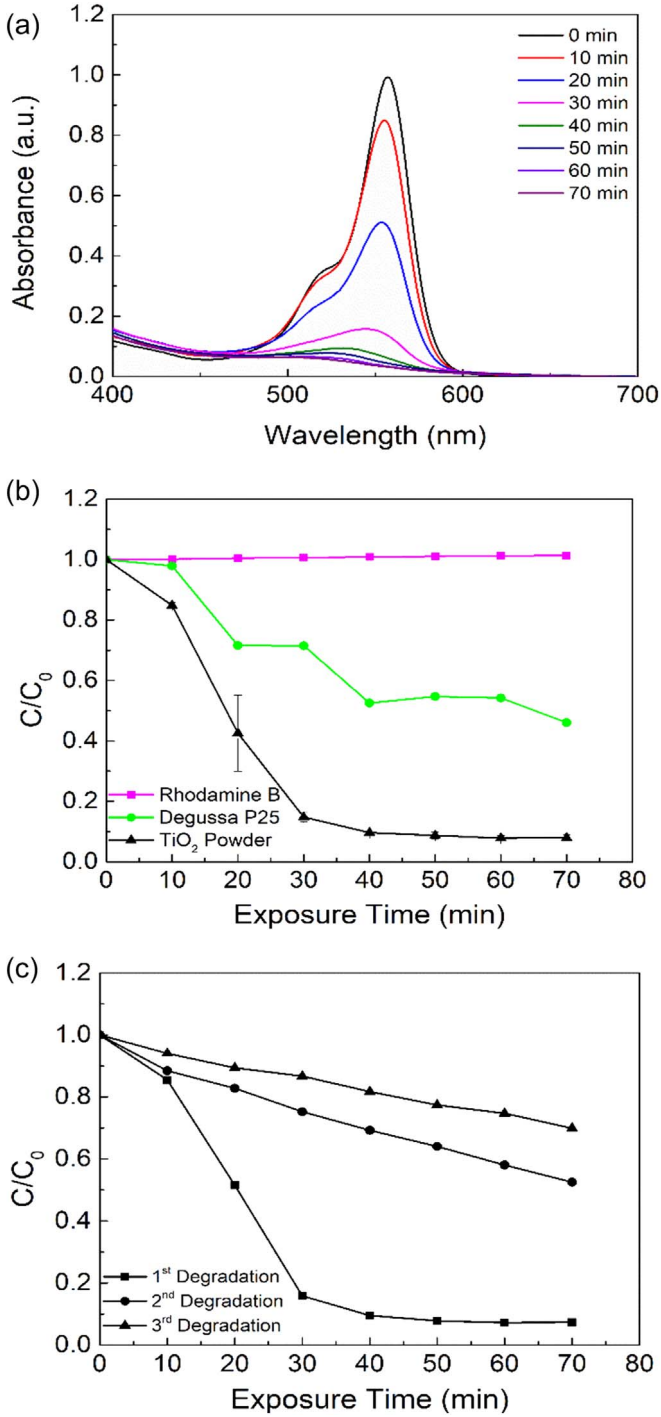


**Figure 5.** Rhodamine B absorbance spectra of the $TiO_2$ nanoparticles at different solar light exposure times up to 70 min (a). Rhodamine B degradation ratio ($C/C_0$) versus solar radiation exposure time, where the blank rhodamine B is also presented (b). Degussa P25 was subjected to the same experiments and is shown for comparison. Three different degradation measurements were carried out for the $TiO_2$ powder material in (b). Several solar radiation exposure experiments were carried out to attest the reusability of the material (c).

(~11 nm). It is known that due to quantum size effect, the nanosized particles display enhanced redox ability. The migration of electrons and holes of smaller particles to their surface is facilitated, and the electron-hole recombination is reduced which increases the photocatalytic performance [67]. Thus, it is expected a substantial size contribution to the enhanced photocatalytic activity observed. Moreover, in general the specific surface area increases with the decrease of particle size [66], also contributing to the behaviour observed.

In terms of crystalline phases, XRD, Raman, and SEM (figures 1 and 3) showed that the microwave synthesis produced $TiO_2$ nanoparticles with mostly anatase and residual amounts of brookite (or impurities). Anatase is largely explored for photocatalytic applications [67], however it has also been reported that a combination of distinct $TiO_2$ phases will result in higher photocatalytic activity and efficiency than single phases [67–69],

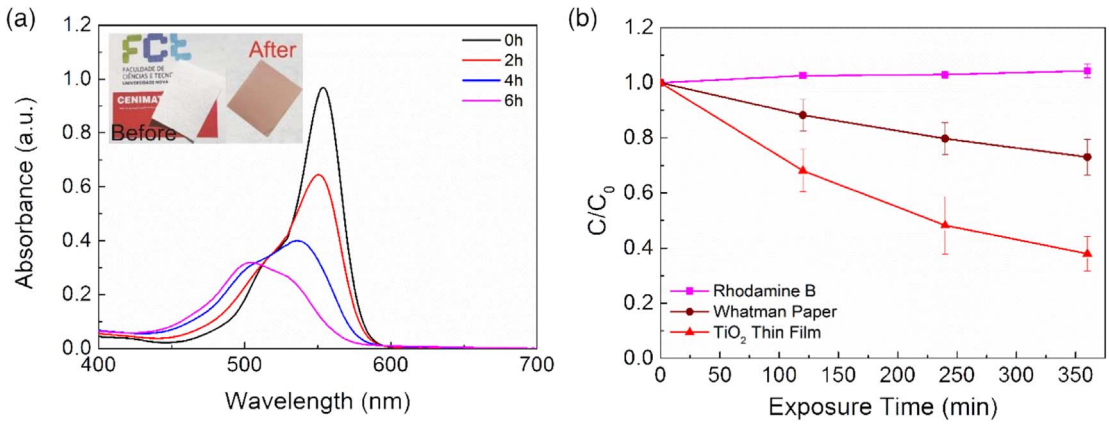


**Figure 6.** Rhodamine B absorbance spectra of the $TiO_2$ nanostructured thin film at different solar light exposure times up to 360 min. Inset shows the photograph of the paper after synthesis and after photocatalysis (a). Rhodamine B degradation ratio ($C/C_0$) versus solar radiation exposure time (b). Three different degradation measurements were carried out for each material.

reducing the recombination of photogenerated holes and electrons [70]. Moreover, the mixture of anatase-brookite nanomaterials has been reported to have higher photocatalytic activity than just anatase or P25 [69, 71, 72]. Thus, some contribution to the photocatalytic performance observed can be expected coming from the mixture of anatase and brookite. Reusability tests were carried out for the $TiO_2$ powder, demonstrating reusability characteristics over time (figure 5(c)). Nevertheless, as can be observed, there is a clear deterioration with the number of photocatalytic experiments [73, 74], which can be related to the powder saturation with rhodamine B [74] or weight loss of the powder during experiments [75]. The blank rhodamine B solution was not significantly influenced under solar radiation, so all the degradation observed is due to the photocatalytic effect of the catalyst in both figures 5 and 6. Nevertheless, it is possible to observe a slight increase in the RhB concentration during exposure to a max of 4% of the initial concentration. This phenomenon can be explained by the evaporation of some of the solvent, which cannot be visible when the photocatalyst is present.

The photocatalytic activity of the $TiO_2$ nanostructured thin film was also studied and is presented in figure 6. The RhB degradation observed in figure 6(a) is accompanied by a slight hypsochromic shift of absorption bands [76], however in figure 6(b), it is clear its gradual degradation under solar radiation up to 6 h.

When comparing the thin film with the powder material (figures 5 and 6), it has been observed that the nanoparticles had a more effective RhB degradation than the nanostructured thin film. This is associated to the better adsorption activity of powders and photocatalytic efficiency when compared to films as a result of the larger surface area and higher amount of material available for reaction [77]. Nevertheless, the nanostructured thin film has reached a degradation value of 68% after 360 min (6 h). As explained for the powder materials, a size effect contribution to the photocatalytic activity can be thought for the film as well. As observed in figure 2, the film is composed by fine nanoparticles agglomerated to form a compact thin film. Several studies described the higher photocatalytic activity of films composed by nanoparticles [78–80], thus as in powder material, it is expected a significant contribution to the observed photocatalytic efficiency coming from the nanosized particles present. Moreover, as can be seen in figure 6(a), the 3D structure of paper contribute to the photocatalytic activity observed [41], associated to partial solution absorption by the Whatman paper which can be observed by the pinkish coloration on it after degradation (see inset in figure 6(a)). The contribution coming from Whatman paper absorption is expected to be ~27% of the total RhB degradation, thus the RhB photodegradation value of 68% is the joint contribution of Whatman paper and the $TiO_2$ nanostructured thin film.

Regarding the phase's contribution, both nanoparticles and nanostructured thin film must have the same crystalline phases, even if it could not be seen clearly in figure 3 due to the cellulose signal contribution, hindering some $TiO_2$ bands. Thus, mixture of $TiO_2$ phases must have contributed to the enhanced photocatalytic performance just as observed for the powder material. The photocatalytic performance obtained by the nanostructured thin film is largely superior when compared to an analogous studies [6], mostly due to the structural differences observed. Thus, it can be stated that the microwave synthesis parameters selected and acid amount demonstrated to be of great importance to the final photocatalytic activity of the materials produced.

The materials were designed to be a reliable alternative for the commercial photocatalysts used nowadays, and to produce fully disposable materials, that can effectively contribute to the environmental protection, while diminishing production costs. The photocatalytic paper developed in the present study can easily be employed

as filters or several other applications, as it easily adapts to different surfaces due to its highly flexibility, despite its green character.

## 4. Conclusions

$TiO_2$ nanoparticles and nanostructured thin films were simultaneously produced using a hydrothermal method assisted by microwave irradiation. Whatman paper has been selected as substrate for the thin film due to its lack of impurities. All materials were composed by a mixture of anatase and brookite polymorphs, with brookite appearing as a minor phase or impurity. It has been observed very fined particles appearing as spheres, that were also observed in the thin film. The nanostructured thin film revealed to be a compact film of agglomerated nanoparticles. Photocatalytic activity was evaluated with the rhodamine B degradation, with the nanoparticles showing the highest photocatalytic activity under solar radiation (91% after 40 min) and revealing reusability characteristics over time. The nanoparticles revealed to have around 12 times higher photocatalytic activity when compared to the commercial Degussa P25 photocatalyst. The nanostructured thin film demonstrated also enhanced photocatalytic performance reaching 68% of RhB degradation after 6 h of solar radiation exposure. The present study showed that this approach is a real and appealing option for the commercial photocatalysts and capable of producing disposable and inexpensive photocatalytic materials in flexible and green substrates.

## Acknowledgments

This work is funded by National Funds through the FCT - Fundação para a Ciência e a Tecnologia, I.P., under the scope of the project UIDB/50025/2020-2023. The authors acknowledge Fundação para a Ciência e a Tecnologia for funding the Project ICARUS under the reference PTDC/EAM-AMB/30989/2017. The work was also partially funded by the Nanomark collaborative project between INCM (Imprensa Nacional - Casa da Moeda) and CENIMAT/i3N. A. C. Marques acknowledges funding to the National Foundation for Science and Technology, I P, through the PhD Grants SFRH/BD/115173/2016. Thanks are also due to EC project SYNERGY H2020-WIDESPREAD-2020-5, CSA, proposal n° 952169. The authors also acknowledge funding from the European Research Council through the Starting Grant TREND, grant 716510 and from the European Community's H2020 program under grant agreement No. 787410 (ERC-2018-AdG DIGISMART).

## Data availability statement

All data that support the findings of this study are included within the article (and any supplementary files).

## Additional information

## Competing financial interests

The authors declare no competing financial interests.

## ORCID iDs

M Matias https://orcid.org/0000-0003-3667-6830
A C Marques https://orcid.org/0000-0001-6878-1040
A Pimentel https://orcid.org/0000-0003-1236-9262
P Barquinha https://orcid.org/0000-0002-5446-2759
E Fortunato https://orcid.org/0000-0002-4202-7047
R Martins https://orcid.org/0000-0002-1997-7669
D Nunes https://orcid.org/0000-0003-3115-6588

## References

[1] Kates R W, Parris T M and Leiserowitz A A 2016 What is sustainable development? Goals, indicators, values, and practice *Enviroment Sci. Policy Sustain. Dev.* **47** 8–21
[2] Sarkis J 2001 Manufacturing's Role in Corporate Environmental Sustainability *I. J. Operations & Production Management* **21** 666–86
[3] O'Brien C 1999 Sustainable production—a new paradigm for a new millennium *Int. J. Prod. Econ.* **60** 1–7

[4] Griggs D, Stafford-Smith M, Gaffney O, Rockström J, Öhman M C, Shyamsundar P, Steffen W, Glaser G, Kanie N and Noble I 2013 Sustainable development goals for people and planet *Nature* **495** 305–7

[5] Zinke R K and Werkheiser W H 2014 Critical mineral resources of the United States—economic and environmental geology and prospects for future supply: U.S. Geological Survey Professional paper 1802 *Encycl. Toxicol.* 3rd Edn (United States of America: USGS) 797

[6] Matias M L, Nunes D, Pimentel A, Ferreira S H, Borda D'Agua R, Duarte M P, Fortunato E and Martins R 2019 Paper-based nanoplatforms for multifunctional applications *J. Nanomater.* 6501923

[7] Nunes D, Pimentel A, Pinto J V, Calmeiro T R, Nandy S, Barquinha P, Pereira L, Carvalho P A, Fortunato E and Martins R 2016 Photocatalytic behavior of $TiO_2$ films synthesized by microwave irradiation *Catal. Today* **278** 262–70

[8] You J, Guo Y, Guo R and Liu X 2019 A review of visible light-active photocatalysts for water disinfection: features and prospects *Chem. Eng. J.* **373** 624–41

[9] Haider A J, Jameel Z N and Al-Hussaini I H M 2019 Review on: titanium dioxide applications *Energy Procedia* **157** 17–29

[10] Aboulouard A, Gultekin B, Can M, Erol M, Jouaiti A, Elhadadi B, Zafer C and Demic S 2020 Dye sensitized solar cells based on titanium dioxide nanoparticles synthesized by flame spray pyrolysis and hydrothermal sol-gel methods: a comparative study on photovoltaic performances *J. Mater. Res. Technol.* **9** 1569–77

[11] Bai F-Q, Li W and Zhang H-X 2017 Theoretical Studies of Titanium Dioxide for Dye-Sensitized Solar Cell and Photocatalytic Reaction *Titanium Dioxide* (Croatia: IntechOpen) (https://doi.org/10.5772/intechopen.68745)

[12] Dar M I, Chandiran A K, Grätzel M, Nazeeruddin M K and Shivashankar S A 2014 Controlled synthesis of $TiO_2$ nanoparticles and nanospheres using a microwave assisted approach for their application in dye-sensitized solar cells *J. Mater. Chem.* A **2** 1662–7

[13] Diasanayake M A K L, Senadeera G K R, Sarangika H N M, Ekanayake P M P C, Thotawattage C A, Divarathne H K D W M N R and Kumari J M K W 2016 $TiO_2$ as a low cost, multi functional material *Mater. Today Proc.* **3** S40–7

[14] Nunes D, Freire T, Barranger A, Vieira J, Matias M, Pereira S, Pimentel A, Cordeiro N J A, Fortunato E and Martins R 2020 $TiO_2$ nanostructured films for electrochromic paper based-devices *Appl. Sci.* **10** 1200

[15] Dinh N N, Oanh N T T, Long P D, Bernard M C and Goff A H L 2003 Electrochromic properties of $TiO_2$ anatase thin films prepared by a dipping sol-gel method *Thin Solid Films* **423** 70–6

[16] Di Paola A, Bellardita M and Palmisano L 2013 Brookite, the least known $TiO_2$ photocatalyst *Catalysts* **3** 36–73

[17] López de Dicastillo C, Guerrero Correa M, Martínez F B, Streitt C and José Galotto M 2020 Antimicrobial effect of titanium dioxide nanoparticles *Antimicrobial Resistance - A One Health Perspective* (Croatia: IntechOpen) (https://doi.org/10.5772/intechopen.90891)

[18] Armelao L, Barreca D, Bottaro G, Gasparotto A, Maccato C, Maragno C, Tondello E, Štangar U L, Bergant M and Mahne D 2007 Photocatalytic and antibacterial activity of $TiO_2$ and Au/$TiO_2$ nanosystems *Nanotechnology* **18** 375709

[19] Joost U, Juganson K, Visnapuu M, Mortimer M, Kahru A, Nõmmiste E, Joost U, Kisand V and Ivask A 2015 Photocatalytic antibacterial activity of nano-$TiO_2$ (anatase)-based thin films: effects on *Escherichia coli* cells and fatty acids *J. Photochem. Photobiol. B Biol.* **142** 178–85

[20] Guo Q, Zhou C, Ma Z and Yang X 2019 Fundamentals of $TiO_2$ photocatalysis: concepts, mechanisms, and challenges *Adv. Mater.* **31** 1–26

[21] Reyes-Coronado D, Rodríguez-Gattorno G, Espinosa-Pesqueira M E, Cab C, De Coss R and Oskam G 2008 Phase-pure $TiO_2$ nanoparticles: anatase, brookite and rutile *Nanotechnology* **19** 145605

[22] Nunes D, Pimentel A, Santos L, Barquinha P, Fortunato E and Martins R 2017 Photocatalytic $TiO_2$ nanorod spheres and arrays compatible with flexible applications *Catalysts* **7** 60

[23] Luttrell T, Halpegamage S, Tao J, Kramer A, Sutter E and Batzill M 2015 Why is anatase a better photocatalyst than rutile? - Model studies on epitaxial $TiO_2$ films *Sci. Rep.* **4** 4043

[24] Andersson M, Österlund L, Ljungström S and Palmqvist A 2002 Preparation of nanosize anatase and rutile $TiO_2$ by hydrothermal treatment of microemulsions and their activity for photocatalytic wet oxidation of phenol *J. Phys. Chem.* B **106** 10674–9

[25] Kawahara S I T, Konishi Y, Tada H, Tohge N and Nishii J 2002 A Patterned $TiO_2$ (Anatase)/$TiO_2$ (Rutile) bilayer-type junction on the photocatalytic activity *Angew. Chemie.* **41** 2811–3

[26] Ameta R, Solanki M S, Benjamin S and Ameta S C 2018 Photocatalysis *Advanced Oxidation Processes for Waste Water Treatment* (United Kingdom: Elsevier) 75–135

[27] Lan Y, Lu Y and Ren Z 2013 Mini review on photocatalysis of titanium dioxide nanoparticles and their solar applications *Nano Energy.* **2** 1031–45

[28] Kalyanasundaram K 2013 Photochemical applications of solar energy: Photocatalysis and photodecomposition of water. *Photochemistry* (41) (Cambridge, UK: The Royal Society of Chemistry) (https://doi.org/10.1039/9781849737722-00182)

[29] Fujishima A and Zhang X 2006 Titanium dioxide photocatalysis: present situation and future approaches *Comptes Rendus Chim.* **9** 750–60

[30] Schneider J, Matsuoka M, Takeuchi M, Zhang J, Horiuchi Y, Anpo M and Bahnemann D W 2014 Understanding $TiO_2$ photocatalysis: mechanisms and materials *Chem. Rev.* **114** 9919–86

[31] Nakata K and Fujishima A 2012 $TiO_2$ photocatalysis: design and applications *J. Photochem. Photobiol. C Photochem. Rev.* **13** 169–89

[32] Subramaniam M N, Goh P S, Lau W J, Ng B C and Ismail A F 2018 Development of nanomaterial-based photocatalytic membrane for organic pollutants removal *Advanced Nanomaterials for Membrane Synthesis and its Applications* (United Kingdom: Elsevier) 45–67

[33] Fresno F, Portela R, Suárez S and Coronado J M 2014 Photocatalytic materials: recent achievements and near future trends *J. Mater. Chem.* A **2** 2863–84

[34] Rueda-Marquez J J, Levchuk I, Fernández Ibañez P and Sillanpää M 2020 A critical review on application of photocatalysis for toxicity reduction of real wastewaters *Journal of Cleaner Production* **258** 120694

[35] Nyamukamba P, Okoh O, Mungondori H, Taziwa R and Zinya S 2018 Synthetic methods for titanium dioxide nanoparticles: a review *Titanium Dioxide - Material for a Sustainable Environment* (Croatia: IntechOpen) (https://doi.org/10.5772/intechopen.75425)

[36] Seifried S, Winterer M and Hahn H 2000 Nanocrystalline titania films and particles by chemical vapor synthesis *Chem. Vap. Depos.* **6** 239–44

[37] Taziwa R and Meyer E 2017 Fabrication of $TiO_2$ nanoparticles and thin films by ultrasonic spray pyrolysis: design and optimization *Pyrolysis* (Croatia: IntechOpen) (https://doi.org/10.5772/67866)

[38] Akpan U G and Hammed B H 2010 The advancements in sol–gel method of doped-TiO2 photocatalysts *Appl. Catal. A: General* **375** 1–11

[39] Liu N, Chen X, Zhang J and Schwank J W 2014 A review on $TiO_2$-based nanotubes synthesized via hydrothermal method: formation mechanism, structure modification, and photocatalytic applications *Catal. Today* **225** 34–51

[40] Periyat P, Leyland N, McCormack D E, Colreavy J, Corr D and Pillai S C 2010 Rapid microwave synthesis of mesoporous $TiO_2$ for electrochromic displays *J. Mater. Chem.* **20** 3650–5

[41] Nunes D, Pimentel A, Araujo A, Calmeiro T R, Panigrahi S, Pinto J V, Barquinha P, Gama M, Fortunato E and Martins R 2018 Enhanced UV flexible photodetectors and photocatalysts based on $TiO_2$ nanoplatforms *Top. Catal.* **61** 1591–606

[42] Joubert T H, Bezuidenhout P H, Chen H, Smith S and Land K J 2015 Inkjet-printed Silver Tracks on Different paper Substrates *Mater. Today Proc.* **2** 3891–900

[43] Kraus W and Nolze G 1996 POWDER CELL—a program for the representation and manipulation of crystal structures and calculation of the resulting x-ray powder patterns *J. Appl. Crystallogr.* **29** 301–3

[44] Villars P and Calvert L D 1986 *Pearson's handbook of crystallographic data for intermetallic phases* (Michigan: American Society for Metals)

[45] Schneider C A, Rasband W S and Eliceiri K W 2012 NIH Image to ImageJ: 25 years of image analysis *Nat. Methods* **9** 671–5

[46] Standard I 2010 Determination of photocatalytic activity of surfaces in an aqueous medium by degradation of methylene blue Iso 10678:2010(E) *Int. Stand.* **2010** 1–18 (https://www.iso.org/standard/46019.html)

[47] Ceballos-Chuc M C, Ramos-Castillo C M, Alvarado-Gil J J, Oskam G and Rodríguez-Gattorno G 2018 Influence of brookite impurities on the raman spectrum of $TiO_2$ anatase nanocrystals *J. Phys. Chem. C* **122** 19921–30

[48] Cullity B D 1956 *Elements of x-ray diffraction* (United States of America: Addison-Wesley Publishing Company) (https://doi.org/10.1119/1.1934486)

[49] Stagi L, Carbonaro C M, Corpino R, Chiriu D and Ricci P C 2015 Light induced $TiO_2$ phase transformation: correlation with luminescent surface defects *Phys. Status Solidi Basic Res.* **252** 124–9

[50] Zhang Q, Ma L, Shao M, Huang J, Ding M, Deng X, Wei X and Xu X 2014 Anodic oxidation synthesis of one-dimensional $TiO_2$ nanostructures for photocatalytic and field emission properties *J. Nanomater.* - 831752

[51] Vásquez G C, Peche-Herrero M A, Maestre D, Alemán B, Ramírez-Castellanos J, Cremades A, González-Calbet J M and Piqueras J 2014 Influence of Fe and Al doping on the stabilization of the anatase phase in $TiO_2$ nanoparticles *J. Mater. Chem.* C **2** 10377–85

[52] Castellanos-Leal E L, Acevedo-Peña P, Güiza-Argüello V R and Córdoba-Tuta E M 2017 N and F codoped $TiO_2$ thin films on stainless steel for photoelectrocatalytic removal of cyanide ions in aqueous solutions *Mater. Res.* **20** 487–95

[53] Nezar S, Saoula N, Sali S, Faiz M, Mekki M, Laoufi N A and Tabet N 2017 Properties of $TiO_2$ thin films deposited by rf reactive magnetron sputtering on biased substrates *Appl. Surf. Sci.* **395** 172–9

[54] Wang Y, Li L, Huang X, Li Q and Li G 2015 New insights into fluorinated $TiO_2$ (brookite, anatase and rutile) nanoparticles as efficient photocatalytic redox catalysts *RSC Adv.* **5** 34302–13

[55] Hu Y, Tsai H L and Huang C L 2003 Effect of brookite phase on the anatase-rutile transition in titania nanoparticles *J. Eur. Ceram. Soc.* **23** 691–6

[56] Du Y, Zhang M S, Wu J, Kang L, Yang S, Wu P and Yin Z 2003 Optical properties of $SrTiO_3$ thin films by pulsed laser deposition *Appl. Phys. A Mater. Sci. Process.* **76** 1105–8

[57] Aydın C, Benhaliliba M, Al-Ghamdi A A, Gafer Z H, El-Tantawy F and Yakuphanoglu F 2013 Determination of optical band gap of $ZnO:ZnAl_2O_4$ composite semiconductor nanopowder materials by optical reflectance method *J. Electroceramics.* **31** 265–70

[58] Yu J G, Yu H G, Cheng B, Zhao X J, Yu J C and Ho W K 2003 The effect of calcination temperature on the surface microstructure and photocatalytic activity of $TiO_2$ thin films prepared by liquid phase deposition *J. Phys. Chem.* B **107** 13871–9

[59] Wu J M, Shih H C and Wu W T 2006 Formation and photoluminescence of single-crystalline rutile $TiO_2$ nanowires synthesized by thermal evaporation *Nanotechnology* **17** 105–9

[60] Reddy K M, Manorama S V and Reddy A R 2003 Bandgap studies on anatase titanium dioxide nanoparticles *Mater. Chem. Phys.* **78** 239–45

[61] Pimentel A, Ferreira S H, Nunes D, Calmeiro T, Martins R and Fortunato E 2016 Microwave synthesized ZnO nanorod arrays for UV sensors: a seed layer annealing temperature study *Materials* **9** 299

[62] Enríquez J P and Mathew X 2003 Influence of the thickness on structural, optical and electrical properties of chemical bath deposited CdS thin films *Sol. Energy Mater. Sol. Cells* **76** 313–22

[63] Pereira L, Barquinha P, Fortunato E, Martins R, Kang D, Kim C J, Lim H, Song I and Park Y 2008 High k dielectrics for low temperature electronics *Thin Solid Films* **516** 1544–8

[64] Moma J and Baloyi J 2018 Modified titanium dioxide for photocatalytic applications *Photocatal. - Appl. Attrib.* (Croatia: IntechOpen) (https://doi.org/10.5772/intechopen.79374)

[65] Guo Y, Li H, Chen J, Wu X and Zhou L 2014 $TiO_2$ mesocrystals built of nanocrystals with exposed {001} facets: facile synthesis and superior photocatalytic ability *J. Mater. Chem.* A **2** 19589–93

[66] He J, Du Y, Bai Y, An J, Cai X, Chen Y and Wang P 2019 Nanocomposites with enhanced photocatalytic activity *Molecules.* **24** 1–14

[67] Fu W, Li G, Wang Y, Zeng S, Yan Z, Wang J, Xin S, Zhang L, Wu S and Zhang Z 2017 Facile formation of mesoporous structured mixed-phase (anatase/rutile) $TiO_2$ with enhanced visible light photocatalytic activity *Chem. Commun.* **54** 58–61

[68] Wang H, Gao X, Duan G, Yang X and Liu X 2015 Facile preparation of anatase-brookite-rutile mixed-phase N-doped $TiO_2$ with high visible-light photocatalytic activity *J. Environ. Chem. Eng.* **3** 603–8

[69] Di Paola A, Bellardita M, Ceccato R, Palmisano L and Parrino F 2009 Highly active photocatalytic $TiO_2$ powders obtained by thermohydrolysis of $TiCl_4$ in water *J. Phys. Chem.* C **113** 15166–74

[70] Mutuma B K, Shao G N, Kim W D and Kim H T 2015 Sol-gel synthesis of mesoporous anatase-brookite and anatase-brookite-rutile $TiO_2$ nanoparticles and their photocatalytic properties *J. Colloid Interface Sci.* **442** 1–7

[71] Yu J C, Yu J, Ho W and Zhang L 2001 Preparation of highly photocatalytic active nano-sized $TiO_2$ particles via ultrasonic irradiation *Chem. Commun.* **1** 1942–3

[72] Yu J C, Zhang L and Yu J 2002 Direct sonochemical preparation and characterization of highly active mesoporous $TiO_2$ with a bicrystalline framework *Chem. Mater.* **14** 4647–53

[73] Wang R, Cai X and Shen F 2013 Preparation of $TiO_2$ hollow microspheres by a novel vesicle template method and their enhanced photocatalytic properties *Ceram. Int.* **39** 9465–70

[74] Nagaveni K, Sivalingam G, Hegde M S and Madras G 2004 Solar photocatalytic degradation of dyes: high activity of combustion synthesized nano $TiO_2$ *Appl. Catal. B Environ.* **48** 83–93

[75] Chen L, Yang S, Mäder E and Ma P C 2014 Controlled synthesis of hierarchical $TiO_2$ nanoparticles on glass fibres and their photocatalytic performance *Dalt. Trans.* **43** 12743–53

[76] Chen F, Zhao J and Hidaka H 2003 Highly selective deethylation of Rhodamine B: adsorption and photooxidation pathways of the dye on the $TiO_2/SiO_2$ composite photocatalyst *Int. J. Photoenergy* **5** 209–17

[77] Chen Y H and Tu K J 2012 Thickness dependent on photocatalytic activity of hematite thin films *I. J. Photoenergy* 980595

[78] Huang J, He Y, Wang L, Huang Y and Jiang B 2017 Bifunctional Au@$TiO_2$ core–shell nanoparticle films for clean water generation by photocatalysis and solar evaporation *Energy Convers. Manag.* **132** 452–9
[79] Liqiang J, Xiaojun S, Weimin C, Zili X, Yaoguo D and Honggang F 2003 The preparation and characterization of nanoparticle $TiO_2$/Ti films and their photocatalytic activity *J. Phys. Chem. Solids* **64** 615–23
[80] Alrousan D M A, Dunlop P S M, McMurray T A and Byrne J A 2009 Photocatalytic inactivation of *E. coli* in surface water using immobilised nanoparticle $TiO_2$ films *Water Res.* **43** 47–54